

Adaptation of microbial resource allocation affects modeled long term soil organic matter and nutrient cycling

Thomas Wutzler^a, Sönke Zaehle^{a,b}, Marion Schrumpf^a, Bernhard Ahrens^a,
Markus Reichstein^{a,b}

^a*Max Planck Institute for Biogeochemistry, Hans-Knöll-Straße 10, 07745 Jena, Germany*

^b*Michael Stifel Center Jena for Data-driven and Simulation Science, Jena, Germany*

Abstract

In order to understand the coupling of carbon (C) and nitrogen (N) cycles, it is necessary to understand C and N-use efficiencies of microbial soil organic matter (SOM) decomposition. While important controls of those efficiencies by microbial community adaptations have been shown at the scale of a soil pore, an abstract simplified representation of community adaptations is needed at ecosystem scale.

Therefore we developed the soil enzyme allocation model (SEAM), which takes a holistic, partly optimality based approach to describe C and N dynamics at the spatial scale of an ecosystem and time-scales of years and longer. We explicitly modelled community adaptation strategies of resource allocation to extracellular enzymes and enzyme limitations on SOM decomposition. Using SEAM, we explored whether alternative strategy-hypotheses can have strong effects on SOM and inorganic N cycling.

Results from prototypical simulations and a calibration to observations of an intensive pasture site showed that the so-called revenue enzyme allocation strategy was most viable. This strategy accounts for microbial adaptations to

both, stoichiometry and amount of different SOM resources, and supported the largest microbial biomass under a wide range of conditions. Predictions of the SEAM model were qualitatively similar to models explicitly representing competing microbial groups. With adaptive enzyme allocation under conditions of high C/N ratio of litter inputs, N in formerly locked in slowly degrading SOM pools was made accessible, whereas with high N inputs, N was sequestered in SOM and protected from leaching.

The findings imply that it is important for ecosystem scale models to account for adaptation of C and N use efficiencies in order to represent C-N couplings. The combination of stoichiometry and optimality principles is a promising route to yield simple formulations of such adaptations at community level suitable for incorporation into land surface models.

Keywords: soil, enzyme, model, stoichiometry, adaptation, microbe

1. Introduction

The global element cycles of carbon (C) and nitrogen (N) are strongly linked and cannot be understood without their intricate interactions (Thorn-ton et al., 2007; Janssens et al., 2010; Zaehle and Dalmonech, 2011). The ties between nutrient cycles are especially strong in the dynamics of soil organic matter (SOM), because the depolymerisation and mineralisation of SOM relies on a microbial decomposer community with a rather strict homeostatic regulation of their stoichiometry, i.e. their elemental ratio of C/N (Sturner and Elser, 2002; Zechmeister-Boltenstern et al., 2015). Therefore, it is important to represent effects of microbial control on soil biogeochemistry also in ecosystem to global scale models (Todd-Brown et al., 2012; Xu et al., 2014).

12 Imbalance fluxes of C and N comprise portions of respiration of organic
13 C, mineralization of organic N, and immobilization of inorganic N. They oc-
14 cur if decomposers experience stoichiometric imbalance, i.e. differences in
15 elemental composition between food and the requirement of feeders (Sturner
16 and Elser, 2002). Decomposers require a certain amount of C for each unit
17 of N. With balanced growth, i.e. when stoichiometry of the food matches
18 the requirements, decomposers can utilize all food for productive purposes
19 such as synthesis of new biomass or enzymes, growth respiration, and main-
20 tenance respiration. If there is different amount of C per unit N in the food,
21 decomposers have to deal with this imbalance.

22 Decomposers can - in principle - adjust in three different ways when faced
23 with imbalances between the stoichiometry of the organic material (OM), i.e.
24 the litter and SOM they feed on, and their own stoichiometric requirements
25 (Mooshammer et al., 2014b). First, individual microbes can adapt their
26 carbon-use efficiency (CUE), or their nutrient-use efficiency (NUE) (Sins-
27 abaugh et al., 2013). The alteration of CUE has shown to have large conse-
28 quences on prediction of carbon sequestration in SOM (Allison, 2014; Wieder
29 et al., 2013). Regulation of nutrient use efficiency has consequences for nutri-
30 ent recycling and loss of nutrients from the ecosystem (Mooshammer et al.,
31 2014a) and soil plant feedback (Rastetter, 2011). Second, decomposer com-
32 munities can adapt their stoichiometric requirements. Community composi-
33 tion can shift between species with high C/N ratio, such as many fungi, or
34 species with lower C/N ratio, such as many bacteria (Cleveland and Liptzin,
35 2007; Xu et al., 2013), although the flexibility is very narrow. Third, de-
36 composers can adapt their allocation of resources into synthesis of different

37 extracellular enzymes to preferentially degrade fractions of SOM that differ
38 by their stoichiometry (Moorhead et al., 2012).

39 Representation and consequences of stoichiometry on element cycling dif-
40 fer between models at different scales. Most models at ecosystem scale em-
41 ploy the first decomposer option, and use changes in CUE or nutrient use
42 efficiency to represent stoichiometric controls on respiration and mineraliza-
43 tion fluxes (Manzoni et al., 2008). However, modelling studies at the pore
44 scale have demonstrated the important effect of community adaptation and
45 their emerging effects on element cycling (Allison and Vitousek, 2005; Resat
46 et al., 2011; Wang et al., 2013). Explicit representation of competition among
47 several microbial groups that differ in their expression of different enzymes
48 resulted in a comparable simulated CUE across a wide range of litter stoi-
49 chiometry (Kaiser et al., 2014). Likely, therefore, there is a need to capture
50 the effects of community adaptation also in models at ecosystem scale.

51 At least two alternatives exist to represent the effects of microbial di-
52 versity at the ecosystem scale. First, competition of several microbial pop-
53 ulations can be explicitly modelled to represent stoichiometric effects such
54 as sustained sequestration of N with high N inputs (Perveen et al., 2014).
55 Second, adaptation of effective properties of the entire microbial community,
56 such as investments into nutrient uptake (Rastetter et al., 1997; Rastetter,
57 2011), can represent the emerging effects in an abstract, but dynamic and
58 adaptive way. The adaptation of enzyme allocation was recently formalised
59 using the second strategy by the conceptual EEZY model (Moorhead et al.,
60 2012) and further developed using the EnzMax allocation strategy by (Aver-
61 ill, 2014). While these models show strong strategy effects on nutrient cycling

62 in time scale of days to months, they do not represent feedback mechanisms
63 to the size and stoichiometry of the SOM pools, and therefore they cannot
64 study the consequences for decadal SOM dynamics.

65 In this paper, we adopt the second alternative of representing microbial
66 diversity as working hypothesis and propose a holistic scheme to represent
67 effects of microbial adaptation of enzyme synthesis on SOM cycle at the
68 ecosystem scale. Our aim was to tackle the need of capturing the decadal
69 time scale effects of adaptive enzyme synthesis on SOM dynamics and nutri-
70 ent recycling. We therefore extended the EEZY model to explore different
71 consequences of alternative enzyme allocation strategies.

72 This paper first introduces the SEAM model (Section 2.1), a dynamical
73 model of SOM cycling that explicitly represents microbial strategies of pro-
74 ducing several extracellular enzyme pools (Section 2.3). Next, the effects of
75 those strategies on SOM cycling are presented by prototypical examples (Sec-
76 tions 2.4 and 3.1). Finally, a calibration to an intensive pasture site (Section
77 2.5) demonstrates the usability of the model (Section 3.2) and compares its
78 predictions to the ones of the Symphony model (Perveen et al., 2014), which
79 explicitly models several microbial-groups.

80 **2. Methods**

81 *2.1. Soil Enzyme Allocation Model (SEAM)*

82 The dynamic Soil Enzyme Allocation Model (SEAM) allows exploring
83 consequences of enzyme allocation strategies for SOM cycling at the soil
84 core to ecosystem from monthly to decadal scale. The modelled system are
85 C and N pools in SOM in a representative elemental volume of soil. The

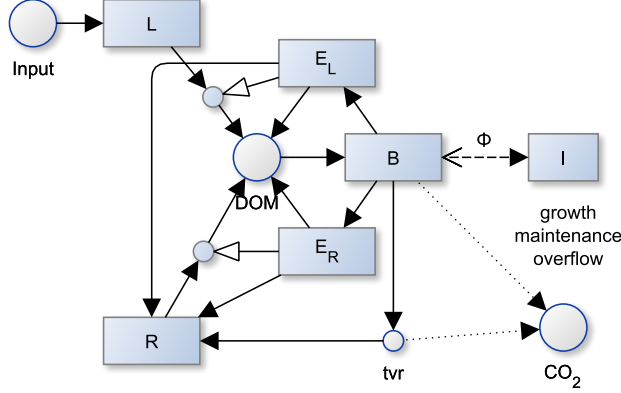


Figure 1: Model structure of SEAM: Two substrate pools (L and R) which differ in their elemental ratios are depolymerized by respective enzymes (E_L and E_R). The simple organic compounds (DOM) are taken up by the microbial community and used for synthesizing new biomass (B), new enzymes, or for catabolic respiration. Turnover of microbial biomass (tvr) is in part mineralized and the rests adds to the residue pool. Stoichiometric imbalance between DOM and B causes overflow respiration or mineralization/immobilization (Φ_B) of inorganic N (I) (further detailed in Fig. 2). Boxes correspond to pools, disks to fluxes, black arrow heads to mass fluxes, white arrow heads to other controls. Solid lines represent fluxes of both C and N, while dotted and dashed lines represent separate C or N fluxes respectively.

86 system could be soil of a laboratory incubation or a layer of a soil profile,
 87 e.g. its upper 20 cm. The model represents different SOM pools containing
 88 C and N as state variables and specifies differential equations for the mass
 89 fluxes. It is driven by C and N inputs of plant litter (both above-ground and
 90 rhizodeposition), inorganic N inputs from deposition and fertilisers, as well
 91 as prescribed uptake of inorganic N by roots. SEAM computes output fluxes
 92 of heterotrophic respiration and leaching of inorganic N.

93 Key features are: first, the representation of several SOM pools that
 94 differ by their stoichiometry, and second, the representation of enzymes that
 95 degrade specifically those SOM pools. The quality spectrum is modelled

Table 1: State variables and input with initial values and input fluxes. Values refer to the Laqueuille pasture calibration.

Symbol	Definition	Value	Unit	Rational
L	C in litter	571	g m^{-2}	quasi steady state
L_N	N in litter	8.15	g m^{-2}	(Perveen et al., 2014) (by their N/C ratio β)
R	C in residue substrate	10500	g m^{-2}	(Allard et al., 2007) (total stocks - L - dR)
R_N	N in residue substrate	968	g m^{-2}	by C/N ratio in (Perveen et al., 2014)
E_L	C in enzymes targeting L	0.34	g m^{-2}	quasi steady state
E_R	C in enzymes targeting R	0.20	g m^{-2}	quasi steady state
B	microbial biomass C	89.2	g m^{-2}	quasi steady state
I	inorganic N	2.09	g m^{-2}	(Perveen et al., 2014)
input_L	litter C input	969.16	$\text{g m}^2\text{yr}^{-1}$	(Perveen et al., 2014) ($m_p C_p^{obs}$)
i_I	inorganic N input	22.91	$\text{g m}^2\text{yr}^{-1}$	(Perveen et al., 2014)
k_{IP}	inorganic plant N uptake	16.04	$\text{g m}^2\text{yr}^{-1}$	(Perveen et al., 2014) (assuming plant steady state: plant N export + litter N input)

by two classes: a C rich litter pool, L , and a N rich pool that consists of microbial residues, R (Fig. 1). Although both pools contain C as well as N, for brevity we sometimes refer to the enzymes degrading the N-rich residue pool as N-degrading enzymes, E_R , and those degrading the C-rich litter pool as C-degrading enzymes, E_L . The most important assumptions are described in the following paragraphs, while the symbols are explained in Tab. A.5 and detailed model equations are provided with Appendix A.

Decomposition of the litter and residue pools follows an inverse Michaelis-Menten kinetics (Schimel and Weintraub, 2003), which is first-order to the

105 amount of OM, and saturates with the amount of the respective enzyme.
 106 C/N ratios, β , of the decomposition flux are equal to the C/N ratios of the
 107 decomposed pool. The C/N ratios of biomass and enzymes are assumed to be
 108 fixed, while those of the substrate pools may change over time due to changing
 109 C/N ratio of total influxes to these pools. Imbalances in stoichiometry of
 110 uptake and microbial requirements are compensated by overflow respiration
 111 or N mineralization. This means that if there is more C in uptake than can
 112 be used based on other constraints, such as available N, it will be respired.
 113 and if there is more N in uptake than can be used by other constraints, such
 114 as available C, it will be mineralized. Total enzyme allocation is a fixed
 115 fraction, a_E , of the microbial biomass, B , per time. However, the microbial
 116 community can use different strategies to adjust their allocation to synthesis
 117 of alternative kinds of new enzymes (Section 2.3). All decomposition fluxes
 118 first fuel a pool of dissolved OM (DOM). This dynamics of this pool is usually
 119 much faster than the dynamics of the other pools. Therefore, SEAM is
 120 simplified by assuming the DOM pool to be in quasi steady state (Wutzler
 121 and Reichstein, 2013). Hence, the sum of all influxes to the DOM pool, i.e.
 122 decomposition plus part of the enzyme turnover, is taken up by the microbial
 123 community and the DOM pool is not simulated explicitly. If expenses for
 124 maintenance and enzyme synthesis cannot be met, the microbial community
 125 starves and declines in biomass.

126 2.2. *Exchange with inorganic N pools*

127 The imbalance flux, Φ_B (A.12c), lets microbes mineralise excess N, or im-
 128 mobilise required N up to a maximum rate, $u_{\text{imm,Pot}}$. The latter is assumed
 129 to increase linearly with the inorganic N pool. While this stoichiometric

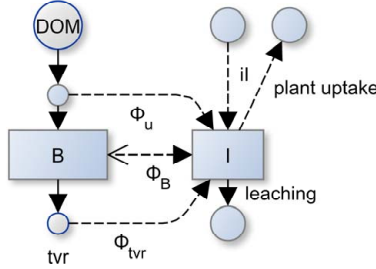


Figure 2: In addition to the maybe negative imbalance flux, Φ_B of microbial biomass, B , there are additional mineralization fluxes feeding the inorganic pool, I , due to mineralization during uptake, Φ_u , and mineralization during microbial turnover, Φ_{tvr} adding up to total mineralization/immobilization flux $\Phi = \Phi_u + \Phi_B + \Phi_{tvr}$. The N dynamics depends also on fluxes across the system boundary, namely input of organic N with litter, input of inorganic N iI , leaching, and plant uptake of inorganic N.

130 imbalance flux is the most widely implemented flux mechanism between mi-
 131 crobial biomass and the inorganic N pools in SOM models (Manzoni and
 132 Porporato, 2009), it is not sufficient to recycle N to the inorganic pool if
 133 microbial biomass is itself N limited. Therefore, two additional mineralisa-
 134 tion fluxes are implemented in SEAM (Fig. 2). First, a fraction of microbial
 135 uptake N in DOM, Φ_u (termed uptake mineralisation), is mineralised to rep-
 136 resent the subscale imbalance flux at C-limited spots of a heterogeneous soil
 137 volume, which is in total not C-limited (Manzoni et al., 2008). Second, a
 138 fraction of microbial turnover is mineralised that accounts for grazing. Graz-
 139 ers respire a fraction of the grazed biomass C to meet their energy demand,
 140 and - assuming invariant grazer stoichiometry - must release an equivalent
 141 amount of nutrients. This mineralization component, here termed turnover
 142 mineralization Φ_{tvr} , has been formalised in the soil microbial loop hypothesis
 143 (Clarholm, 1985; Raynaud et al., 2006).

144 In the light of the introduction of these additional N mineralisation fluxes,

Table 2: Increasing levels of N limitation

Term		Definition
Organic N lim.		N in microbial uptake of organic matter is less than constrained by other elements ($\Phi_B < 0$).
Microbial N lim.		uptake of organic matter plus maximum immobilisation flux is not enough to satisfy microbial N requirements ($-\Phi_B \geq u_{\text{imm,Pot}}$).
Decomposer system N lim.		There is a net transfer from the inorganic pool to the organic pools ($\Phi = \Phi_B + \Phi_u + \Phi_{\text{tvr}} < 0$).

145 a refinement of the term N-limitation in modelling concepts (Table 2) is re-
 146 quired. When microbes cannot meet their stoichiometric demand by DOM
 147 uptake but can meet their demand by immobilising inorganic N, we suggest
 148 the term *organic N limitation*. When the immobilisation flux cannot meet the
 149 stoichiometric requirement of the microbial community, we suggest the term
 150 *microbial N-limitation*. Despite the maximum microbial immobilisation flux
 151 there might still be a net mineralization in the system due to uptake mineral-
 152 ization and turnover mineralization. When there is a net N immobilization
 153 in the system, i.e. a net transfer from the inorganic pool to the organic pools
 154 of SOM and microbial biomass, we suggest the term *decomposer system N*
 155 *limitation*. While the two first terms are relevant for microbial ecology, the
 156 last term is controlling N availability for plants.

Table 3: Microbial enzyme allocation strategies

Strategy	Allocation is
Fixed	independent, constant
Match	adjusted to achieve balanced growth, i.e. β_{DOM} matches microbial demands
EnzMax	corresponds to Match-Allocation if microbial N-limited, and to $\alpha = 0.5$ otherwise
Revenue	proportional to return per investments into enzymes

157 2.3. Enzyme allocation strategies

158 Microbes allocate a proportion α of their total enzyme investments, $a_e B$,
159 to the synthesis of enzymes targeting the N-rich R substrate and a proportion
160 $1 - \alpha$ to the synthesis of enzymes targeting the N-poor, but better degradable
161 L substrate (1).

$$\text{syn}_{E_R} / (\text{syn}_{E_R} + \text{syn}_{E_L}) \equiv \alpha \quad (1)$$

162 Four different strategies of allocating investments among synthesis of al-
163 ternative enzymes were explored in this study (Table 3).

164 The **Fixed** strategy assumes that allocation is independent of, and not
165 changing with changes in substrate availability.

$$\alpha = \text{const.} = 1/2 \quad (2)$$

166 This strategy corresponds to the models without enzyme allocation adapta-
167 tion where decomposition rate is a function of microbial biomass (Wutzler
168 and Reichstein, 2008).

169 The **Match** strategy assumes that microbes regulate enzyme synthesis
170 in a way that the decomposition products balance their stoichiometric de-
171 mands (Moorhead et al., 2012). The partitioning coefficient α (1) is derived
172 by equating the C/N ratio of the sum of uptake fluxes after other expenses,
173 such as growth and maintenance respiration, to the C/N ratio of microbial
174 biomass, β_B . The equation of (Moorhead et al., 2012) has been adapted
175 to take into account inorganic N immobilization and to an "anabolic" mi-
176 crobial efficiency rather than an carbon use efficiency lumping growth and
177 maintenance respiration.

$$\beta_B = \frac{\epsilon(\text{dec}_L + \text{dec}_R - r_M)}{\text{dec}_L / \beta_L + \text{dec}_R / \beta_R - \Phi_M}, \quad (3)$$

178 where dec_L , and dec_R are depolymerisation fluxes of the litter and residue
179 pools, respectively (A.4), which both are a function of enzyme levels and,
180 hence, indirectly a function of α . r_M is maintenance respiration (A.2b), ϵ is
181 the anabolic microbial efficiency accounting for growth respiration (A.7), β_i
182 are C/N ratios of the respective pools i , and Φ_M is the net flux of N from
183 living microbes to the mineral N pool. Equation 3 for simplicity neglects the
184 small inputs of enzymes to DOM. Here, we assume that microbes use the
185 maximal immobilisation of inorganic N, $u_{\text{imm,Pot}}$ (A.9) to meet their stoichio-
186 metric requirements with the Match strategy. Hence, the net N imbalance
187 flux is the difference between mineralization during uptake and the immobili-
188 sation: $\Phi_M = \Phi_u - u_{\text{imm,Pot}}$. With microbial N-limitation, (3) has no solution.
189 In this case, the enzyme effort is allocated entirely to the N-rich substrate
190 ($\alpha = 1$), and excess carbon uptake is respired by overflow respiration.

191 If current enzyme pools E_S , are assumed to be in quasi steady-state with

192 their respective substrate $S \in \{L, R\}$ and microbial biomass, then equation
 193 3 can be solved for partitioning coefficient, α .

$$\alpha_M = f_{\alpha\text{Fix}}(L, \beta_L, R, \beta_R, E_L, E_R, r_M, \Phi_M) \quad (4a)$$

$$\alpha = \begin{cases} 0, & \text{if } \alpha_M \leq 0 \\ 1, & \text{if } \alpha_M \geq 1 \\ \alpha_M, & \text{otherwise} \end{cases} \quad (4b)$$

194 where the long equation (4a) is given with supplementary material together
 195 with R-code and the SYMPY script of its derivation. The bound to one is
 196 necessary to handle the case of microbial N-limitation. The bound to zero
 197 corresponds to the theoretical case where the C-rich substrate may not suffice
 198 to cover microbial C demands relative to N demands.

199 The **ExtMax** strategy (Averill, 2014) matches stoichiometry if microbes
 200 are substrate N limited, and uses a fixed allocation coefficient $\alpha = 0.5$ if
 201 microbes are not substrate N-limited, i.e. C-limited. In order to avoid frequent
 202 jumps between the two cases, a weighted mean between the two fluxes was
 203 used for N imbalance fluxes near $\Phi_b = 0$ with α approaching α_M for N
 204 mineralization or approaching 0.5 for N immobilization indicating substrate-
 205 C limitation.

206 The **Revenue** strategy assumes that the microbial community adapts in
 207 a way to ensure that the investment into enzyme synthesis is proportional to
 208 its revenue, i.e. the return per investment regarding the currently limiting
 209 element:

$$\alpha_C = \frac{\text{rev}_{RC}}{\text{rev}_{LC} + \text{rev}_{RC}} \quad (5a)$$

$$\alpha_N = \frac{\text{rev}_{RN}}{\text{rev}_{LN} + \text{rev}_{RN}}, \quad (5b)$$

210 where rev_S is the revenue from given substrate $S \in \{L, R\}$ with microbial
 211 C and N-limitation respectively. The revenue is computed on the current
 212 status quo, i.e. the current enzyme levels. Appendix Appendix B argues
 213 why investing proportional into all enzymes is better than investing into the
 214 single best enzyme. The return is the current decomposition flux from the
 215 substrate degraded by the respective enzyme (A.4), and the assumed invest-
 216 ment balances enzyme turnover to keep current enzyme levels, E_S^* (A.3).

$$\text{rev}_{SC} = \frac{\text{return}}{\text{investment}} = \frac{\text{dec}_{S,Pot} \frac{E_S^*}{K_{M,S} + E_S^*}}{k_{NS} E_S^*} = \frac{\text{dec}_{S,Pot}}{k_{NS} (K_{M,S} + E_S^*)} \quad (6a)$$

$$\text{rev}_{SN} = \frac{\text{dec}_{S,Pot} \frac{E_S^*}{K_{M,S} + E_S^*} / \beta_S}{k_{NS} E_S^* / \beta_E} = \text{rev}_{SC} \frac{\beta_E}{\beta_S}, \quad (6b)$$

217 where k_{NS} is rate of enzyme turnover, $K_{M,S}$ is enzyme's substrate affinity,
 218 $\text{dec}_{S,Pot}$ is enzyme saturated decomposition flux (A.4), and β are C/N ratios
 219 of the respective pools.

220 There are two resulting partitioning coefficients, α_C and α_N with C or
 221 N-limited microbial biomass, respectively. In order to avoid frequent large
 222 jumps under near co-limitation, SEAM implements a smooth transition be-
 223 tween these two cases as a weighted average.

Table 4: Prototypical simulation experiments

Experiment	Explored issue
VarN-Incubation	Efficiency of using given fixed substrate levels that vary by N content
Substrate-feedback	Possibility and size of steady state substrate pools
Priming	Increased substrate decomposition and mineralization after a pulse addition of fresh litter
CO ₂ -Fertilization	Continued increase of litter C inputs but constant litter N inputs

$$\alpha = \frac{w_{\text{CLim}}\alpha_C + w_{\text{NLim}}\alpha_N}{w_{\text{CLim}} + w_{\text{NLim}}}, \quad (7)$$

where w is the strength of the limitation of the respective element, specifically the ratio of required to available biomass synthesis fluxes (A.13).

2.4. Prototypical simulation experiments

Several prototypical simulation experiments (Table 4) were used to explore the consequences of the different microbial enzyme allocation strategies (2.3) for the simulated SOM dynamics. They increase in complexity from a soil incubation experiment to a decadal CO₂ manipulation treatment. All experiments used parameter values given in Table A.5 unless stated otherwise in this section. For the prototypical experiments, the inorganic N pool was kept constant at $I = 0.4 \text{ gN m}^{-2}$, while inorganic N feedbacks were considered in Section 2.5.

235 The **VarN-Incubation** experiment explored to which efficiency sub-
 236 strates of given a stoichiometry are used for microbial biomass growth with
 237 the different enzyme allocation strategies. A simplified model version was
 238 used in this experiment, where all the inputs and feedback to the substrate
 239 pools (L and R) were neglected, and in which these pools were kept constant
 240 ($dL/dt = dR/dt = 0$). This simplification led to a quasi steady state of
 241 microbial biomass and enzyme levels for the given substrate supply. This
 242 experiment mimics a short-term incubation experiment, where changes in
 243 litter and residue pools are negligible small. The assumed boundary condi-
 244 tions for this experiment were fixed substrate carbon of $L = 100 \text{ gC m}^{-2}$, and
 245 $R = 400 \text{ gC m}^{-2}$. The C/N ratio of the residue pool was assumed constant at
 246 $\beta_R = 7$, whereas litter C/N ratio varied between 18 and 42 ($\beta_L = [18, \dots, 42]$).

247 The **Substrate-feedback** experiment explored the decadal trajectories
 248 of the entire system including feedback to the substrate pools. Litter input
 249 was assumed constant at a rate of $\text{input}_L = 400 \text{ gC m}^{-2}\text{yr}^{-1}$ with a C/N
 250 ratio of $\beta_{\text{input}_L} = 30$.

251 The **Priming** experiment explored the effect of rhizosphere priming, i.e
 252 the input of fresh litter into a bulk subsoil. Specifically, the simulations
 253 evaluated the fluxes after an addition of 50 gC and a respective amount of
 254 N (C/N ratio $\beta_{\text{input}_L} = 30$) on a soil that otherwise received a litter input
 255 of only $30 \text{ gC m}^{-2}\text{yr}^{-1}$ (and respective N with $\beta_{\text{input}_L} = 30$) for a decade.
 256 The assumption is made that the rhizodeposition litter input (both pulse and
 257 continuous) was very easily degradable litter, specifically with a maximum
 258 turnover of $k_L = 10 \text{ day}^{-1}$. The amendmend was simulated by a single pulse,
 259 i.e. a step change in the litter pool.

260 The **CO₂-Fertilization** experiment explored the effect of increased con-
 261 tinuous litter C input, which is expected with elevated atmospheric CO₂
 262 concentration. The simulations started from steady state corresponding to
 263 initial litter C input of $\text{input}_L = 400 \text{ gC m}^{-2}\text{yr}^{-1}$, applied 20% increased C
 264 inputs during years 10 to 60, and applied initial litter inputs again during the
 265 next 50 years. The litter N inputs were kept constant over time, implying
 266 an increase in the litter C/N ratio of 20%. Litter input rate was assumed
 267 constant across the year.

268 *2.5. Calibration to a fertilised pasture site*

269 To test the capacity of SEAM to simulate the net carbon storage of a
 270 pasture site including feedback of the inorganic N pool, we calibrated the
 271 model to data of an intensive pasture. The intensive pasture calibration was
 272 tackled only with the Revenue strategy, because the Match and the EnzMax
 273 strategies had already shown inadequate for scenarios including feedbacks to
 274 substrate pools during in the Substrate-feedback experiment. The control
 275 case of the Fixed strategy did not allow for adaptation of microbial enzyme
 276 allocation.

277 The model drivers and most of the parametrisation and drivers (Tables
 278 A.5 and 1) were taken from Perveen et al. (2014). The site is a temperate
 279 permanent pasture located at an altitude of 1040m a.s.l. in France (Laque-
 280 uille, 45°38'N, 2°44'E), receives an annual precipitation of 1200 mm and has
 281 an annual mean temperature of 7 °C.

282 The N-balance of the fertilised pasture is characterised by very high in-
 283 organic N-inputs. A fraction of this N is sequestered in accumulating SOM,
 284 a fraction is lost to leaching, while the remainder is exported with plant

285 biomass harvest. Plant uptake of inorganic N was computed as the sum of
286 plant litter production and plant biomass exports, keeping the plant N pool
287 constant.

288 Model parameters were chosen corresponding to Table 1 in Perveen et al.
289 (2014), and initial litter and SOM pools were prescribed to observed val-
290 ues. Three parameters were calibrated: the maximum decomposition rates
291 of substrate pools, k_L and k_R , and the anabolic carbon-use efficiency, ϵ . Ini-
292 tial pools of microbial biomass and enzymes were set to the decadal steady
293 state in order to prevent large transient initial fluctuations in model pools.
294 The calibration used the *optim* function from R *stats* package (R Core Team,
295 2016) and minimised the differences between model predictions and observa-
296 tions normalised by the standard deviation of the observations. The calibra-
297 tion used observations of the litter OM, the inorganic N, leaching, and rate
298 of change of the total SOM pool ($\approx dR/dt$ if L is near quasi steady state).

299 Subsequently, the calibrated parameters were used to generate predictions
300 for several scenarios of altered inputs to the system.

301 The R-code to generate the results and figures of this paper is available
302 upon request.

303 **3. Results**

304 First, the results of several prototypical artificial simulation experiments
305 clarify the general behaviour and features of the SEAM model. Next, results
306 of a parameter calibration demonstrate the model’s ability to simulate the
307 observed C and N dynamics of an intensive pasture and explore feedbacks
308 with the dynamics of the inorganic N pool.

309 3.1. Prototypical simulation experiments

310 Under the **VarN-Incubation** experiment, in which the substrate pools
311 were fixed, there were marked differences in the effect of allocation strategies
312 on simulated biomass and the imbalance flux (Fig. 3).

313 The Match strategy allowed balanced growth, and yielded the highest
314 substrate efficiency and lowest mineralization fluxes among the enzyme allo-
315 cation strategies. Across a range of litter C/N ratios of 22 to 42 the match
316 strategy yielded non-positive imbalance fluxes, i.e. no mineralization of ex-
317 cess N or overflow respiration of excess C. This means, that microbes could
318 utilize all food taken up for productive expenditures. However, the match
319 strategy also yielded lowest biomass among the strategies. In the discussion
320 we argue that this means an inferior strategy.

321 With the Revenue strategy, enzyme allocation also varied with litter N
322 content, but to a lesser extent. With litter containing enough N (low C/N
323 ratio), still about 5% of the enzyme synthesis C expenditures were allocated
324 into R degrading enzymes. This resulted in higher mineralization of excess
325 N, but in turn allowed for a higher microbial biomass. With high C/N
326 ratio of litter, investment into R-degrading enzymes increased to about 30%,
327 much less than with the Match strategy. Hence, the Revenue strategy yielded
328 higher overflow respiration associated with a low carbon-use efficiency (CUE),
329 but gained more of the limiting element N with the decomposition flux.

330 The Fixed strategy yielded higher N-mineralization due to stoichiometric
331 imbalance at low C/N ratios. At high C/N ratios its constant allocation coef-
332 ficient was intermediate between the other strategies, leading to intermediate
333 values of all the other outputs.

334 The EnzMax strategy was equal to the Match strategy with low C/N
335 ratios, equal to the Fixed strategy with high C/N ratios, and a transition
336 between those two at C/N ratios around 23.

337 When the substrate pools were allowed to be refuelled by microbial and
338 enzyme turnover with the **Substrate-feedback** experiment, both Fixed and
339 the Revenue strategies caused substrate pools to approach a steady state.
340 However, the microbes with Match strategy solely degraded the stoichiomet-
341 rically better matching high-N residue pool, R . Hence, they declined together
342 with the R residues pool despite the large amount of N accumulating in the
343 stoichiometrically less favourable litter pool (Fig. 4). Similarly, with Enz-
344 Max strategy L pools accumulated until microbes became C limited. Then
345 there was an unreasonable explosion like increase of microbial biomass, un-
346 til this L accumulated L pool had been degraded. Because of the Match
347 and the EnzMax strategies yielded unreasonable behaviour when including
348 feedback to substrate pools in the model, they were omitted in the following
349 simulation experiments.

350 When the soil was amended with a pulse of litter with the **Priming ex-**
351 **periment**, a clear true priming effect, i.e. an increased decomposition of
352 the existing SOM, was simulated with the Fixed and Revenue strategy. The
353 priming effect occurred due to a strong enhancement of residue decompo-
354 sition (Fig. 5). This enhancement was stronger with the Revenue strat-
355 egy than with the Fixed strategy, primarily because of a higher simulated
356 microbial biomass with the Revenue strategy. In consequence, also the N -
357 mineralization flux due to microbial turnover was larger with the Revenue
358 strategy (Fig. 5). Note, that the time scale of the simulated priming effect

359 of more than 100 days was longer than observed in priming experiments.

360 When the continuous litter C input was assumed to be higher for 50
361 years with the **CO₂-fertilisation experiment**, enzyme allocation strategies
362 yielded marked difference in SOM stocks (Fig. 6) and nutrient recycling
363 (Fig. 7). While litter stocks, L , increased with both strategies following
364 the increased input, the residues stock, R , slightly increased with the Fixed
365 strategy, but declined strongly with the Revenue strategy. This was the
366 consequence of an increased mining of the R pool with the Revenue strategy.
367 Accordingly, N mineralization was much stronger with the Revenue strategy
368 during elevated CO₂ period, with largest contribution from mineralization by
369 microbial turnover. In this experiment the microbes were organic N limited
370 ($\Phi_B < 0$), but the decomposer system was not N limited, i.e. there was a total
371 N flux towards the plant accessible inorganic N pool ($\Phi_u + \Phi_B + \Phi_{\text{tvr}} > 0$).
372 The adaptive Revenue strategy in effect helped plants to liberate more N
373 from SOM under elevated CO₂ in the following way. There was a transfer
374 from SOM R pool to living biomass to microbial turnover that was in part
375 mineralized. The turnover of the increased microbial biomass returned more
376 N to the mineral N pool than taken up by immobilization flux of living
377 microbes. The increased mineral N pool helped plants to grow. However,
378 this response was transient. After litter inputs returned to initial values, the
379 system recovered towards the initial state but only on centennial time scale
380 that would even be longer if prescribing a longer turnover time for slower
381 SOM pools.

382 3.2. *Intensive pasture simulation*

383 The calibrated SEAM model successfully simulated the observed C and
384 N balance of the Laqueuille intensive pasture (Figure 8). In contrast to the
385 prototypical simulation experiments, here, the feedback of the inorganic N
386 pool was included, the model was driven and compared to observed values,
387 and only the Revenue strategy has been considered.

388 The observed continuous build-up of an organic N pool in the residue
389 SOM was driven by the system’s positive N balance. Two pathways caused
390 the model behaviour in SEAM. First, inorganic N was taken up by the plant
391 and returned to the soil via organic N in litter. Second, microbial biomass
392 immobilised inorganic N due to its stoichiometric imbalance with the sub-
393 strate. The microbial biomass was N-limited when only considering uptake
394 of organic substrate. However, it was C-limited when accounting for immo-
395 bilisation of inorganic N.

396 Simulated alteration of C and N inputs to the system strongly affected the
397 internal SOM and nutrient cycling. Effects were shown by several simulation
398 scenarios that started from the calibrated state but applied a step change in
399 inputs of litter or inorganic N (Figure 9) as detailed in following paragraphs.

400 Increased litter C input by 50% together with an increased litter C/N
401 ratio by 25% (elevated CO₂ scenario) caused a shift in enzyme allocation
402 towards enzymes degrading the N-rich residue pool and an increase of the
403 litter pool. The higher input also increased the mineral N demand of both
404 the plant to balance increased biomass synthesis and the microbial biomass
405 with its higher stoichiometric imbalance. The resulting decrease in mineral N
406 also decreased leaching losses. Moreover, ecosystem available N was re-used

407 more often, because of a higher turnover flux of N in increased microbial
408 biomass.

409 Decreased inorganic N inputs from $22.9 \text{ g m}^{-2}\text{yr}^{-1}$ down to $1 \text{ g m}^{-2}\text{yr}^{-1}$
410 together with a doubling of litter C/N ratio caused a strong shift in enzyme
411 allocation towards enzymes degrading the N-rich residue SOM with similar
412 consequences as with increased C input, such as an increase in litter OM.
413 However, in this scenario, the decreased N inputs caused a depletion of the
414 mineral N pool. As a consequence, the microbial biomass could not use
415 immobilisation to balance substrate stoichiometry and became N-limited.
416 This caused overflow respiration and a decreasing trend in residue SOM.

417 Increased inorganic N inputs from $22.9 \text{ g m}^{-2}\text{yr}^{-1}$ up to $25.6 \text{ g m}^{-2}\text{yr}^{-1}$
418 together with a decrease of litter C/N by 25% did not much affect the system
419 behaviour, because the soil system was already C-limited at the start. The
420 microbial biomass could only immobilise a small fraction of the additional
421 N to build up new SOM. Instead, N accumulated in the inorganic pool with
422 associated increased losses to leaching.

423 4. Discussion

424 Microbial adaptation of enzyme synthesis to substrate availability ben-
425 efited the community so that higher microbial biomass levels could be sus-
426 tained on a wider range of substrate stoichiometry. The different prototypic
427 simulation experiments and the simulation of the intensive pasture led to
428 similar conclusions on the effects of adaptation of enzyme allocation.

4.1. Amounts of substrates matter

The amount of substrate and the substrate stoichiometry are both important for regulating enzyme allocation. The Match strategy failed to account for substrate amount, assuming that microbes can achieve balanced growth under a wide range of substrate stoichiometry (Moorhead et al., 2012; Ballantyne and Billings, 2014). This strategy yielded lower microbial biomass both in the VarN-Incubation (Fig. 3) and in the Substrate-feedback experiments (Fig. 4). We argue that producing less biomass means an inferior strategy, because slower growing microbes have a competitive disadvantage to faster growing microbes that have otherwise same properties such as maintenance requirements. Match-strategy microbes focused on degrading a stoichiometrically balanced, but declining residues pool, leaving the large amount of N available in a stoichiometrically less favourable litter pool untouched (Fig. 4).

Averill (2014) also found that the best microbial allocation strategy maximised growth instead of C or N use efficiency. They found that with C-limitation the best allocation would be strictly equal to all the enzymes. In their study, however, they did not consider feedbacks to the substrate pools, nor immobilization of inorganic N. Moreover, they used a decomposition equation that was completely independent of amount of available substrate. The strategy would allocate the same amount of resources to enzymes that depolymerize a tiny substrate pool as they allocate to enzymes that depolymerize a large substrate pool. Their EnzMax strategy implemented in this study with a different decomposition equation (A.4) led to strange behaviour with buildup of large C-pools with N limitation and sudden switches in en-

zyme allocation and explosive growth of microbial biomass to unreasonable high values until the accumulated amount of litter had been degraded (Fig. 4).

These findings imply that microbial enzyme allocation strategies should account for substrate amounts.

4.2. Community adaptation leads to a more efficient substrate usage

The adaptive Revenue strategy consistently supported higher biomass and had lower N mineralization fluxes at steady state compared to the non-adaptive Fixed strategy with the VarN-Incubation experiment (Fig. 3). Similar patterns appeared with the other experiments (Figs. 4 and 7). Such better substrate usage is in line with results of individual based small-scale modelling (Kaiser et al., 2014). The finding implies that N mineralization fluxes with imbalanced substrates may be lower than inferred from previous modelling studies that did not account for community adaptation.

4.3. Comparison to observed changes in enzyme stoichiometry

The SEAM model focuses on community adaptation of enzyme synthesis. It predicts a change in the ratio of enzyme activities of enzymes degrading C-rich plant litter versus enzymes degrading the N-rich residue SOM when changing inputs of inorganic N to the soil. While only low variation in stoichiometry of N-degrading versus C-degrading enzymatic activity is observed across biomes (Sinsabaugh et al., 2009), microcosm studies detect short-term changes of enzyme activities with N fertilization (Kumar et al., 2016), but their observations differ between different kinds of N-degrading enzymes. Hence, the evidence is mixed.

SEAM also predicts accelerated turnover of the residue pool associated with increased enzyme activity of N-degrading enzymes after increased inputs of litter C in relation to litter N. Such patterns are observed at field scale at Duke forest, where Phillips et al. (2011) found an increased activity of extracellular enzymes involved in breakdown of organic N associated with accelerated SOM turnover after increased root exudation with elevated CO₂. In an artificial root exudation experiments at the same site, Drake et al. (2013) found an increase of N degrading NAG enzyme activity with C-only inputs and a shift from oxidative towards hydrolytic enzymes decomposing low molecular weight (lmw) components with C+N inputs. Assuming that the lmw-components have higher C/N ratios, this observed shift is in line with SEAM predictions.

4.4. *SOM as nutrient bank*

Nitrogen was stored in residue SOM during periods of high N inputs and released during periods of low N inputs relative to C inputs in simulations (Fig. 6). When there was excess litter carbon, the microbial community preferentially depolymerised, or mined, the N-rich residue pool, and thereby made the N available for plants. When carbon inputs were low, microbes degraded the residue pool to a lesser extent, but continued to build new residue via microbial turnover. Hence, under low C conditions, the microbes kept N in the decomposer system instead of releasing it through mineralisation.

This 'bank' mechanism (sensu Perveen et al., 2014) also worked when simulating the intensive pasture (Fig. 9). During simulations of high inorganic N inputs, N was sequestered in SOM at a high rate. With decreased inorganic N inputs, the sequestration rate decreased until it became negative,

that is the N in slower decomposing SOM pools was mined. In the long-term, i.e. centuries, the inputs to the system have to balance the outputs of the system. Hence, in the intensive pasture simulation, inorganic N pools and N leaching increased with the increase of SOM with the SEAM model. The conservation or release of N by the bank mechanism implies greater potential for ecosystems to avoid progressive N limitation (Norby et al., 2010; Franklin et al., 2014; Averill et al., 2015). This finding potentially has consequences on feedbacks of global change, especially on the projected C land uptake (Friedlingstein et al., 2014).

4.5. *Priming effects liberate N*

Priming effects, i.e. the altered decomposition of SOM after soil amendments (Kuzyakov et al., 2000), are a potential mechanism to help plants stimulate N release from the SOM for plant nutrition. Priming effects and associated increased N mineralization were simulated for both, the Fixed and Revenue strategies (Fig. 5). With adaptive microbial enzyme allocation (Revenue strategy), increasing plant litter input or increases in litter C/N upregulated the decomposition of the N-rich residue pool (Fig. 6). This in turn influenced the distribution of N in the ecosystem, and N availability for plants (Fig. 7). This active role of plant inputs has been demonstrated in a soil incubation experiment (Fontaine et al., 2011) and has been further conceptualised with the SYMPHONY model (Perveen et al., 2014). Our results are in line with these studies, although our explanation is on a more abstract level (see Section 4.7).

Mineralization during microbial turnover is important for nutrient recycling. Without the additional mineralization mechanisms of uptake mineral-

528 ization (Manzoni et al., 2008) and turnover mineralization (Clarholm, 1985;
529 Raynaud et al., 2006) in our simulation experiment, microbes shifted enzyme
530 allocation to degrade the residues pool, but the N was then sequestered in
531 microbial biomass and not mineralised to inorganic N. Hence, our simula-
532 tion experiments reinforced the need for representing soil heterogeneity and
533 microbial turnover by grazing for making N available for plants under N
534 limitation.

535 *4.6. Mismatch in time scale of priming effects*

536 The unrealistically long time-scale of the priming effect of several months
537 in SEAM (Fig. 5) resulted from both, the long turnover time of enzymes,
538 and the sustaining positive feedback between amounts of microbial biomass
539 and enzymes. It was in contrast with incubation studies that observe priming
540 effects within days or weeks that rapidly declined after the amendment has
541 been used up (Blagodatskaya et al., 2014). The priming timescale in SEAM
542 was longer than the duration of the uptake pulse of the *L* amendment that
543 only lasted a few days. It was controlled by simulated lifetime of enzymes
544 and enzyme turnover, which SEAM described as first order kinetics with a
545 turnover of about a week. Moreover, the priming timescale was prolonged by
546 the positive feedback of increased microbial biomass producing more enzymes
547 that again fuelled microbial biomass.

548 One possible cause for a shorter priming time-scale is a different dynam-
549 ics of enzyme turnover. However, prescribing a shorter turnover time of en-
550 zymes would require an unrealistically large effort of producing enzymes by
551 microbial biomass. More sophisticated models of different enzyme turnover
552 kinetics including stabilisation of a part of the enzymes on mineral surfaces

553 (Burns et al., 2013) may be able to resolve such contradictions. Testing this
554 hypothesis would require observations of the fraction of C uptake allocated
555 to enzyme synthesis and on age distribution of enzymes in the soil which
556 might be feasible with labelling studies.

557 An alternative cause for a shorter priming time-scale may be an important
558 control of enzyme activity that is not strongly coupled to microbial biomass
559 dynamics. Some enzymes such as peroxidase need to be fuelled by labile OM
560 themselves (Rousk et al., 2014) with no immediate relationship to microbial
561 biomass dynamics. This explanation, however, implies that enzyme activity
562 and decomposition of SOM become largely decoupled from enzyme synthesis
563 and microbial dynamics in the short-term. This option is contrary to the
564 assumption of most current models that simulate the priming effect. Such
565 a fundamental change of model assumption would affect most implications
566 gained from SOM modelling studies that involve soil microbes.

567 Another cause for a shorter priming time-scale, is a diminished sustaining
568 positive feedback between enzymes and microbial biomass. Currently, graz-
569 ing is modelled as an implicit part of a first-order microbial turnover. With
570 increasing microbial biomass, grazers become more efficient (Clarholm, 1981).
571 With implementing a time-lagged stronger increase in microbial turnover rate
572 with microbial biomass, biomass levels would decrease faster to pre-treatment
573 levels and help to shorten the time-scale of the priming effect. Testing this
574 hypothesis requires data on grazing during priming effects.

575 Overall, the mismatch in the time scale of priming between simulations
576 and observations hints to gaps in understanding of short-term SOM turnover.
577 However, this model limitation does not impair the simulated longer-term

578 microbial community controls on SOM cycling both in the prototypic simu-
579 lation and at the pasture site. We argue therefore that the simulated decadal
580 patterns are robust, because they are more strongly controlled by the pro-
581 portions in enzyme synthesis than by the time scale of priming effects.

582 *4.7. A holistic view for upscaling*

583 The presented SEAM model takes a holistic view (Panikov, 2010) of mi-
584 crobial community and their adaptations instead of explicitly describing mi-
585 crobial diversity. In this respect, it differs from the SYMPHONY model
586 (Perveen et al., 2014) and similar models (Fontaine et al., 2003), which ex-
587 plicitly model several microbial groups. However, the effective behaviour
588 of the presented SEAM model is similar to these models. SEAM assumes
589 that community composition is to a large extent driven by external drivers.
590 Specifically, SEAM describes an adaptive allocation of resources into break-
591 down of different substrates by assuming that the community composition
592 adapts to changed substrate availability in a way to balance microbe’s rev-
593 enue of the currently limiting element. While the mechanistic approach of the
594 SYMPHONY model explicitly represents this adaptation by shifts between
595 microbial groups, the holistic approach represents its effects at community
596 level. While the mechanistic approach provides more detailed understanding,
597 the proposed abstraction of microbial competition is a step forward to better
598 represent couplings of soil carbon and nutrient cycles in large-scale ecosys-
599 tem models, as it obviates the need to correctly parameterise the underlying
600 mechanisms.

601 The holistic SEAM model yielded qualitatively similar predictions as the
602 mechanistic SYMPHONY model with simulating priming, the bank mecha-

nism, and a continuous SOM sequestration under high inorganic N inputs. SEAM differed from SYMPHONY in the prediction of the inorganic N pool during low N inputs. Specifically, SEAM predicted a decrease in this pool, while SYMPHONY predicted an increase in this pool due to changed competition (Perveen et al., 2014). The difference is probably caused by different assumptions on how the DOM pool is shared among groups of the microbial community and resulting different competition conditions. In SEAM, decomposition products become mixed in a shared DOM pool, while in the SYMPHONY model the decomposition products are not shared between the microbial groups. The truth at pore scale is in between, in that decomposition products are mainly used by the group that is producing the extracellular enzymes, while a part of the DOM diffuses also to other groups (Kaiser et al., 2014). At larger scales, such details cannot be measured or resolved. The difference in model prediction implies that the rationality of the simplified model assumptions of a mixed DOM pool can be qualitatively tested against observations.

4.8. Testable predictions of change of SOM C/N ratios

The SEAM model can be used to predict decadal patterns of SOM cycling following changes in substrate stoichiometry. Observations of such patterns provide evidence for or against the modelling assumptions. Specifically, SEAM predicted a change in proportions of the litter pool and the SOM pool (Fig. 6). While these abstract pools are not directly comparable to observations, a measurable consequence is the associated change of total SOM C/N ratio at the time scale of turnover of the residue pool. Specifically, SEAM predicted a decline in SOM stocks and an increase of SOM C/N with

628 FACE experiments at formerly C-limited systems over time scales of several
629 decades. Observed accelerated SOM turnover at the Duke forest after 12 years
630 of elevated CO₂ (Drake et al., 2011) is a first indication, although there is
631 a continuum of responses to experimental CO₂ increase across sites.

632 *4.9. Outlook*

633 The biggest limitation of the SEAM model is its focus on a single process:
634 community adaptation of enzyme allocation. In order to focus, we had to
635 ignore several other important processes. One such process is the second mi-
636 crobial community strategy of handling substrate stoichiometric imbalance,
637 the adaptation of stoichiometry of microbial biomass. Although the poten-
638 tial of this biomass adaptation is thought to be quite limited (Mooshammer
639 et al., 2014b), it will need to be tested whether these two strategies can be
640 combined within a model.

641 Next, the optimality principle will be extended to also determine the pro-
642 portion of uptake that is allocated to enzyme synthesis. Presence of cheaters,
643 i.e. microbes that consume substrate but without producing enzymes, effec-
644 tively lower the community-level allocation to enzymes (Kaiser et al., 2014).
645 Community development can be assumed to maximise biomass production.
646 Such an assumption can be used to compute the optimal community en-
647zyme synthesis and allows exploring effects on SOM cycling, such as more
648 constrained carbon and nutrient use efficiencies.

649 Moreover, SEAM will be simplified by assuming quasi-steady state of
650 biomass or enzyme pools (Wutzler and Reichstein, 2013). These simplifi-
651 cations will lead to fewer parameters and improved parameter identifiability
652 in model calibration to observations (Xu et al., 2014). Together with im-

653 plementing the influence of environmental factors such as temperature and
654 moisture (Davidson et al., 2012), these changes will make SEAM more suit-
655 able to be used as a component within larger scale land surface models.

656 5. Conclusions

657 The SEAM model (Fig. 1) provides a holistic description of community
658 adaptations. It yields qualitatively similar predictions as microbial-group-
659 explicit models with the ability to represent priming effects, bank mechanism,
660 and a continuous SOM sequestration with high inorganic N inputs (Fig. 9).
661 Hence, this study is an important step for providing an abstract description
662 of microbial community effects and adaptations, with the long-term goal of
663 including the important mechanisms into earth system models.

664 Adapting the allocation of resources into the synthesis of different en-
665 zymes can be an effective means of the microbial community to react to
666 changing substrate stoichiometry. Allocation adaptation strategies helped
667 the simulated microbial biomass in SEAM to grow larger across a wider
668 range of substrate stoichiometry (Fig. 3). Among the tested strategies, the
669 Revenue strategy, which accounts for the amount of substrate pools and their
670 stoichiometry, was particularly successful. These findings imply that models
671 simulating soil carbon and nutrients dynamics (Fig 5) need to account for
672 adaptations in carbon and nutrient strategies. Accounting for adaptations
673 will be especially important when studying the competition for nutrients be-
674 tween soil microorganism and plants, because SOM can function as a storage
675 to sequester surplus nutrients and prevent them from being lost from the
676 system (Fig. 6 and 7).

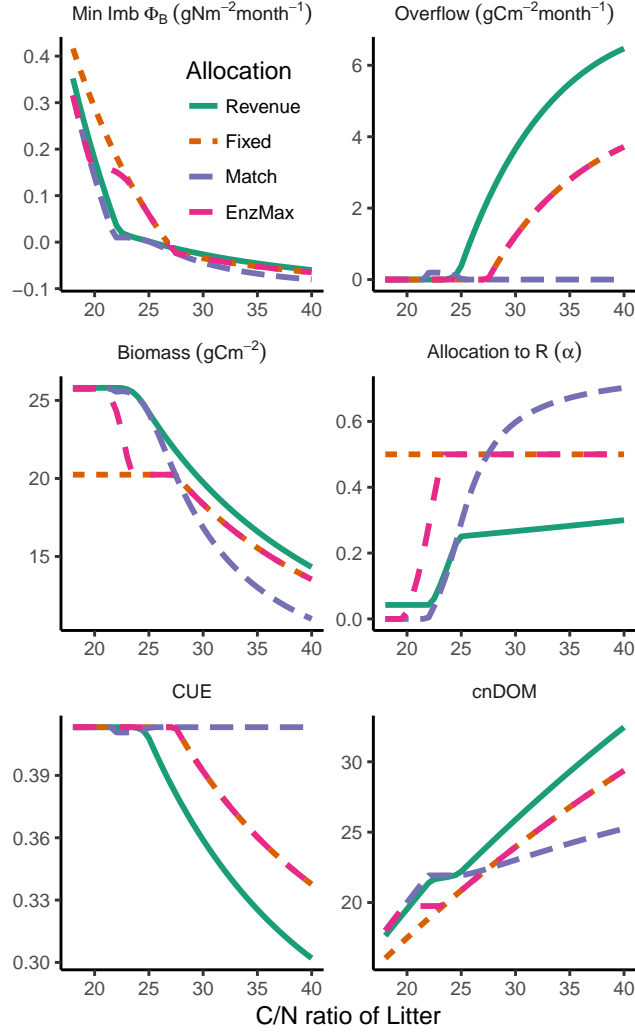


Figure 3: Match enzyme allocations strategy yielded highest resource efficiency, i.e. lowest mineralization fluxes (N mineralization and C overflow respiration) at steady state with the VarN-experiment. Microbes with alternative strategies, however, were more competitive as indicated by a higher biomass. The patterns are caused by different adaptation of resource allocation (α) affecting C/N ratio of the decomposition flux (cnDOM) and carbon use efficiency (CUE).

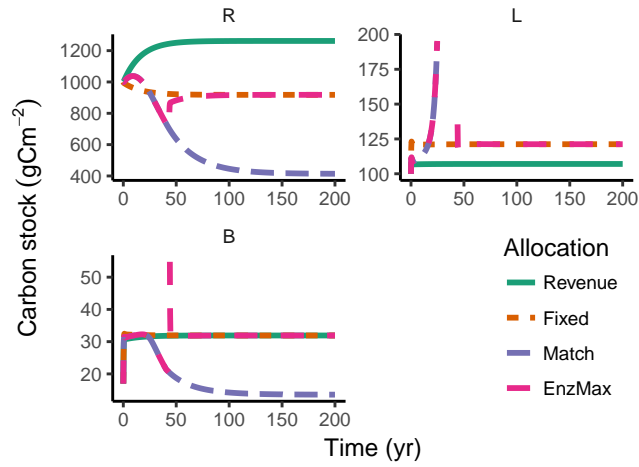


Figure 4: Match strategy was not viable when considering feedback to substrate pools with the SimSteady experiment. Microbes with Match-strategy degraded the stoichiometrically matching but declining R substrate pool and their biomass, B, declined despite the N stores in stoichiometrically less favourable litter, L. Note that range of B and L has been limited and does not display all very large values with the Match and EnzMax strategies.

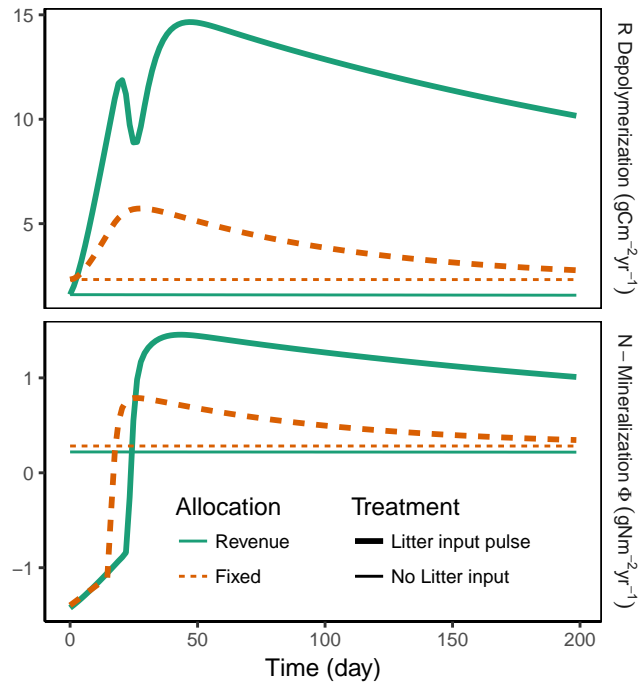


Figure 5: Both depolymerisation of the residue substrate pool and total N mineralization Φ were stimulated most strongly with the Revenue strategy after a subsoil has been amended with a pulse of fresh litter (Priming experiment) compared to a control with no amendment (thin horizontal lines).

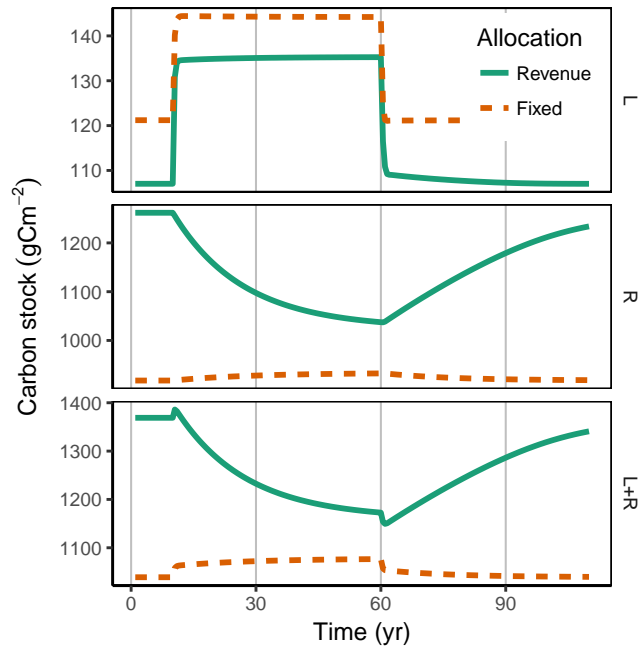


Figure 6: Revenue strategy led to a mining, i.e. decrease, of the residue substrate pool, R , that was stronger than the increase in litter substrate pool, L , during increased carbon litter inputs in years 10 to 60 with the CO_2 -Fertilization experiment.

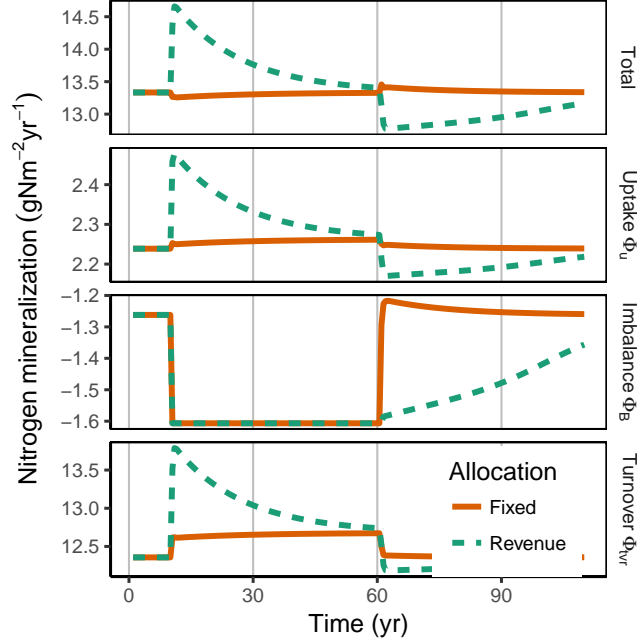


Figure 7: Mineralization of N associated with microbial turnover contributed most of the liberation of SOM-N with the Revenue strategy during CO₂-Fertilisation, which started at year 10. After the end of the fertilisation at year 60, microbes with the Revenue strategy continued to more strongly immobilize N (negative flux Φ_b).

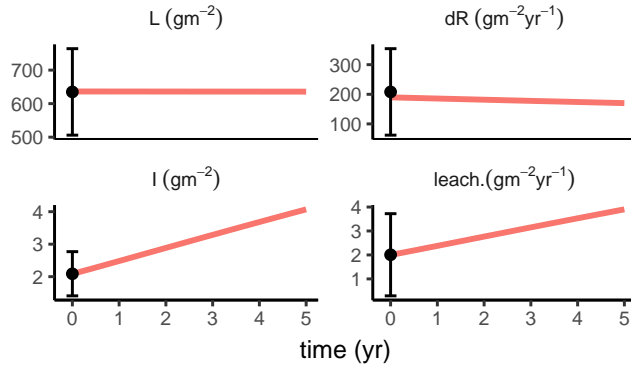


Figure 8: Calibrated SEAM predictions (lines) matched observations from the Laqueuille intensive pasture site (dots and errorbars) of litter pool, L , change of SOM pools, dR , inorganic N, I , and N leaching rate.

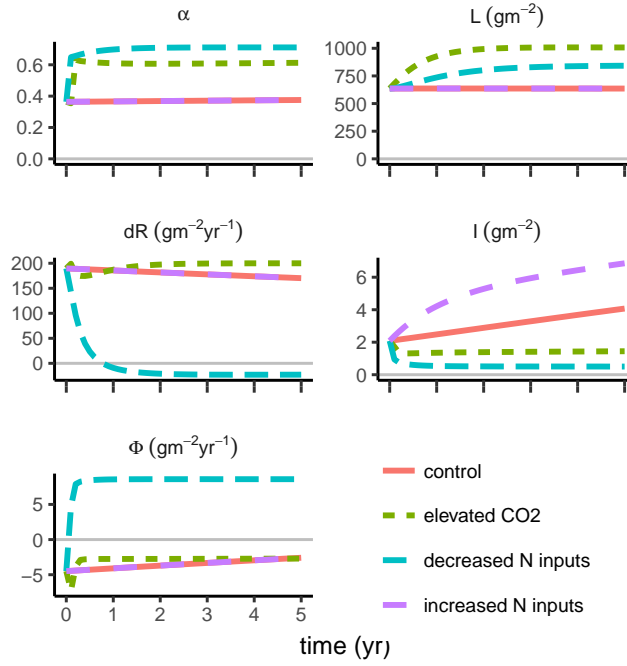


Figure 9: Prescribed alteration of C and N inputs for Laqueuille intensive pasture site led to subsequent simulated shifts in enzyme allocation (α) and affected development of soil pools. Increased N substrate limitation, either due to elevated CO₂ or due to decreasing inorganic N inputs, caused a decrease in mineral N pool, I . If the substrate N limitation could not be balanced by inorganic N input, then the change rate of the residue pool, dR , decreased down to negative values, i.e. decreasing SOM pools.

677 Appendix A. SEAM equations

678 For an overview of symbol definitions see tables 1, A.5, and A.6.

679 Appendix A.1. Carbon fluxes

$$\frac{dB}{dt} = \text{syn}_B - \text{tvr}_B \quad (\text{A.1a})$$

$$\frac{dE_L}{dt} = (1 - \alpha) \text{syn}_E - \text{tvr}_{EL} \quad (\text{A.1b})$$

$$\frac{dE_R}{dt} = \alpha \text{syn}_E - \text{tvr}_{ER} \quad (\text{A.1c})$$

$$\frac{dL}{dt} = -\text{dec}_L + \text{input}_L \quad (\text{A.1d})$$

$$\frac{dR}{dt} = -\text{dec}_R + \epsilon_{\text{tvr}} \text{tvr}_B + (1 - \kappa_E)(\text{tvr}_{ER} + \text{tvr}_{EL}), \quad (\text{A.1e})$$

680 where α is the proportion of total investment into enzymes that is allocated
 681 to the residue pool R (section 2.3, input_L is the litter C input to the system,
 682 ϵ_{tvr}) is the fraction of microbial turnover C that is respired by predators, and
 683 κ_E is the fraction of enzyme turnover that is transferred to the DOM instead
 684 of the R pool. The specific fluxes are detailed below.

Total enzyme production syn_E , maintenance respiration r_M , and micro-
 bial turnover tvr_B are modelled as a first-order kinetics of biomass:

$$\text{syn}_E = a_E B \quad (\text{A.2a})$$

$$r_M = m B \quad (\text{A.2b})$$

$$\text{tvr}_B = \tau B \quad (\text{A.2c})$$

685 Enzyme turnover (tvr_{ER} and tvr_{EL}) is modelled as first-order kinetics of
 686 enzyme levels.

$$\text{tvr}_{ES} = k_E E_S, \quad (\text{A.3})$$

687 where S represents the litter L and residue R substrate pools, respectively.

Substrate depolymerisation is modelled first-order to substrate availability with a saturating Michaelis-Menten kinetics to enzyme levels:

$$\text{dec}_{S,Pot} = k_S S \quad (\text{A.4a})$$

$$\text{dec}_S = \text{dec}_{S,Pot} \frac{E_S}{K_{M,S} + E_S} \quad (\text{A.4b})$$

688 The DOM pool is assumed to be in quasi steady state, and hence, the
 689 sum of all influxes to the DOM pool (decomposition + part of the enzyme
 690 turnover) is taken up by microbial community.

$$u_C = \text{dec}_L + \text{dec}_R + \kappa_E (\text{tvr}_{ER} + \text{tvr}_{EL}) \quad (\text{A.5})$$

691 Under C limitation, C available for synthesis of new biomass and associ-
 692 ated catabolic growth respiration, C_{synBC} , is the difference between C uptake
 693 and expenses for enzyme synthesis (eq. A.2a) and maintenance respiration
 694 (eq. A.2b).

$$C_{\text{synBC}} = u_C - \text{syn}_E / \epsilon - \text{r}_M \quad (\text{A.6})$$

695 If the C balance for biomass synthesis, syn_B (eq. A.11), is positive, only
 696 a fraction ϵ , the anabolic carbon use efficiency (CUE) is used for synthesis
 697 of biomass and enzymes, whereas the rest is used for catabolic growth res-

698 piration r_G to support this synthesis. The model assumes that requirements
699 for enzyme synthesis and maintenance must be met. Hence, the microbial C
700 balance can become negative where microbial biomass starves and declines.

$$\text{syn}_B = \begin{cases} \epsilon C_{\text{synB}}, & \text{if } C_{\text{synB}} > 0 \\ C_{\text{synB}}, & \text{otherwise} \end{cases} \quad (\text{A.7a})$$

$$r_G = \begin{cases} (1 - \epsilon) C_{\text{synB}}, & \text{if } C_{\text{synB}} > 0 \\ 0, & \text{otherwise,} \end{cases} \quad (\text{A.7b})$$

701 where C_{synB} is the C balance for biomass synthesis and is given below by eq.
702 A.11.

703 *Appendix A.2. Nitrogen fluxes*

704 Nitrogen fluxes and pools are derived by dividing the respective fluxes
705 with the C/N ratio, β , of their source.

The C/N ratios β_B and β_E of the microbial biomass and enzymes are assumed to be fixed. However, the C/N ratio of the substrate pools may

change over time and thus the substrate N pools are modelled explicitly.

$$\frac{dL_N}{dt} = -\text{dec}_L / \beta_L + \text{input}_L / \beta_i \quad (\text{A.8a})$$

$$\begin{aligned} \frac{dR_N}{dt} = & -\text{dec}_R / \beta_R + \epsilon_{\text{tvr}} \text{tvr}_B / \beta_B + \\ & (1 - \kappa_E)(\text{tvr}_{ER} + \text{tvr}_{EL}) / \beta_E \end{aligned} \quad (\text{A.8b})$$

$$\frac{dI}{dt} = +i_I - k_{IP} - lI + \Phi \quad (\text{A.8c})$$

$$\Phi = \Phi_u + \Phi_B + \Phi_{\text{tvr}} \quad (\text{A.8d})$$

$$\Phi_u = (1 - \nu)u_{N,OM}, \quad (\text{A.8e})$$

706 where the balance of the inorganic N pool I sums inorganic inputs i_I , plant
 707 uptake k_{IP} , leaching lI , and the exchange flux with soil microbial biomass, Φ .
 708 The latter is the sum of the apparent mineralization due to soil heterogeneity
 709 (Manzoni et al., 2008), Φ_u , mineralisation-immobilisation imbalance flux,
 710 Φ_B (A.12c), and mineralisation of a part of microbial turnover, Φ_{tvr} (A.14b,
 711 section Appendix A.5).

Organic N uptake, $u_{N,OM}$, was modelled as a parallel scheme (PAR), where a part of the organic N that is taken up from DON is mineralised accounting at soil core scale accounting for imbalance flux at sub-scale soil spots with high N concentration in DOM (Manzoni et al., 2008). Potential N uptake is the sum of organic N uptake and the potential immobilisation flux ($u_{\text{imm,Pot}}$). Uptake from DOM is assumed equal to influxes to DOM times

the apparent N use efficiency ν .

$$u_N = \nu u_{N,OM} + u_{\text{imm,Pot}} \quad (\text{A.9a})$$

$$u_{N,OM} = \text{dec}_L / \beta_L + \text{dec}_R / \beta_R + \kappa_E (\text{tvr}_{ER} + \text{tvr}_{EL}) / \beta_E \quad (\text{A.9b})$$

$$u_{\text{imm,Pot}} = i_B I, \quad (\text{A.9c})$$

712 where C/N ratios β_L and β_R are calculated based on current C and N sub-
713 strate pools: $\beta_L = L/L_N$.

The N available for biomass synthesis is the difference of microbial N uptake and expenses for enzyme synthesis. This translates to a N constraint for the C used for biomass synthesis and its associated catabolic growth respiration: $C_{\text{synB}} \leq C_{\text{synBN}}$.

$$N_{\text{synBN}} = u_N - \text{syn}_E / \beta_E, \quad (\text{A.10a})$$

$$C_{\text{synBN}} = \beta_B N_{\text{synBN}} / \epsilon \quad (\text{A.10b})$$

714 *Appendix A.3. Imbalance fluxes of C versus N limited microbes*

715 There are constraints of each element on the synthesis of new biomass
716 and associated growth respiration. The minimum of these fluxes (eq. A.11)
717 constrains the synthesis of new biomass.

$$C_{\text{synB}} = \min(C_{\text{synBC}}, C_{\text{synBN}}) \quad (\text{A.11})$$

The excess elements are lost by imbalance fluxes (eq. A.12). The excess C is respired by overflow respiration, r_O , and the excess N is mineralised,

M_{Imb} , so that the mass balance is closed.

$$r_O = u_C - (\text{syn}_B + \text{syn}_E / \epsilon + r_G + r_M) \quad (\text{A.12a})$$

$$M_{\text{Imb}} = u_N - (\text{syn}_B / \beta_B + \text{syn}_E / \beta_E) \quad (\text{A.12b})$$

$$\Phi_B = M_{\text{Imb}} - u_{\text{imm,Pot}} \quad (\text{A.12c})$$

718 The actual mineralisation-immobilisation flux Φ_B is the difference be-
 719 tween the potential immobilisation flux and excess N mineralization. If
 720 microbes are limited by C availability, Φ_B will be positive, whereas with
 721 substrate N limitation, Φ_B will be a negative flux, corresponding to N immo-
 722 bilisation. With microbial N limitation, i.e. required immobilisation is larger
 723 than potential immobilisation, $\Phi_B = -u_{\text{imm,Pot}}$ and stoichiometry must be
 724 balanced by overflow respiration.

725 *Appendix A.4. Weight of an element limitation*

726 The weight of an element limitation is computed as the ratio between
 727 required uptake flux for given other constraints to the available fluxes for
 728 biosynthesis.

$$w_{\text{CLim}} = \left(\frac{\text{required}}{\text{available}} \right)^\delta = \left(\frac{C_{\text{synBN}}}{C_{\text{synBC}}} \right)^\delta \quad (\text{A.13a})$$

$$w_{\text{NLim}} = \left(\frac{\epsilon C_{\text{synBC}} / \beta_B}{N_{\text{synBN}}} \right)^\delta, \quad (\text{A.13b})$$

729 where parameter δ , arbitrarily set to 200, controls the steepness of the transi-
 730 tion between the two limitations. X_{synBY} denotes the available flux of element

731 X for biosynthesis and associated respiration given the limitation of element
 732 Y (A.6) and (A.10).

733 *Appendix A.5. Turnover mineralization fluxes*

In addition to mineralization flux due to stoichiometric imbalance, a part of microbial biomass is mineralised during microbial turnover, e.g. by grazing. A part $(1 - \epsilon_{\text{tvr}})$ of the biomass is used for catabolic respiration. With assuming that predator biomass elemental ratios do not differ very much from the one of microbial biomass, a respective proportion of N must be mineralized.

$$r_{\text{tvr}} = (1 - \epsilon_{\text{tvr}}) \text{tvr}_B \quad (\text{A.14a})$$

$$\Phi_{\text{tvr}} = (1 - \epsilon_{\text{tvr}}) \text{tvr}_B / \beta_B \quad (\text{A.14b})$$

734 All the non-respired turnover C enters the residue pool. In reality, a part
 735 of the microbial turnover probably enters the DOM pool again (e.g. by cell
 736 lysis) and is taken up again by microbial biomass. The increased uptake
 737 nearly cancels with an increased turnover. Hence, SEAM does not explicitly
 738 consider this shortcut loop so that fewer model parameters are required.
 739 Note, however, that turnover, uptake, and CUE in the model are slightly
 740 lower than in the real system where this shortcut operates.

Table A.5: Model parameters. The two value columns of initial values and parameter values refer to the prototypical examples and the Laqueuille pasture calibration respectively.

Symbol	Definition	Value		Unit	Rational
β_B	C/N ratio of microbial biomass	11	11	g g^{-1}	(Perveen et al., 2014)
β_E	C/N ratio of extracellular enzymes	3.1	3.1	g g^{-1}	(Sturner and Elser, 2002)
β_{input_L}	C/N ratio of plant litter inputs	30	70	g g^{-1}	(Perveen et al., 2014) ($1/\beta$)
k_R	maximum decomposition rate of R	1	4.39e-2	yr^{-1}	calibrated
k_L	maximum decomposition rate of L	5	1.95	yr^{-1}	calibrated
k_E	enzyme turnover rate	60	60	yr^{-1}	(Burns et al., 2013)
κ_E	fraction enzyme tnr. entering DOM instead R	0.8	0.8	(-)	mostly small proteins
a_E	enzyme production per microbial biomass	0.365	0.365	yr^{-1}	$\approx 6\%$ of biomass synthesis
K_M	enzyme half saturation constant	0.05	0.05	g m^{-2}	magnitude of DOC concentration
τ	microbial biomass turnover rate	6.17	6.17	yr^{-1}	(Perveen et al., 2014) (s/ϵ_{tvr})
m	specific rate of maintenance respiration	1.825	0	yr^{-1}	(van Bodegom, 2007), zero in (Perveen et al., 2014)
ϵ	anabolic microbial C substrate efficiency	0.5	0.53	(-)	calibrated
ν	aggregated microbial organic N use efficiency	0.7	0.9	(-)	(Manzoni et al., 2008)
ϵ_{tvr}	microbial turnover that is not mineralized	0.3	0.8	(-)	part of turnover is consumed by predators
i_B	maximum microbial uptake rate of inorganic N	25	25	yr^{-1}	larger than simulated immobilization flux
l	inorganic N leaching rate	-	0.959	yr^{-1}	(Perveen et al., 2014) (l)

Table A.6: Further symbols of quantities derived within the system

Symbol	Definition	Unit
α	proportion of enzyme investments allocated to production of E_R	(-)
syn_B	C for microbial biomass synthesis	$\text{g m}^2\text{yr}^{-1}$
syn_{E_S}	C synthesis of enzymes degrading $S \in \{L, R\}$	$\text{g m}^2\text{yr}^{-1}$
tvr_B	microbial biomass turnover C	$\text{g m}^2\text{yr}^{-1}$
tvr_{E_S}	enzyme turnover C	$\text{g m}^2\text{yr}^{-1}$
dec_S	C in decomposition of resource $S \in \{L, R\}$	$\text{g m}^2\text{yr}^{-1}$
u_C, u_N	microbial uptake of C and N	$\text{g m}^2\text{yr}^{-1}$
$\Phi_u, \Phi_B, \Phi_{\text{tvr}}, \Phi$	N mineralization with microbial DOM uptake, stoichiometric imbalance, turnover, and total $\Phi = \Phi_u + \Phi_B + \Phi_{\text{tvr}}$ (Fig. 2)	$\text{g m}^2\text{yr}^{-1}$

741 **Appendix B. Revenue strategie’s rational**

742 This section explains the rational in a bit more detail, why the allocation
743 proportional to the revenue is optimal from a community perspective.

744 For a single microbe it would be optimal to maximise growth by investing
745 all resources in that enzyme that maximises the return per investment for
746 the currently limiting element. Hence, it should allocate all resources to
747 the enzymes yielding the maximum revenue. However, if many microbes
748 compete for the same best substrate, they also have to share the return of the
749 extracellular decomposition process. If another microbe targets the second-
750 best substrate by producing a different set of enzymes, it does not need to
751 share the returns. When taking this competition into account, it makes sense
752 to allocate the most resources for the best revenue but also some resources
753 to the other possibilities. Hence, the revenue strategy allocates resources
754 proportional to their revenue.

755 *Acknowledgements* We thank Nazia Perveen and Sébastien Fontaine for
756 letting us reuse the data that they used for fitting the SYMPHONY model.
757 TW acknowledges support from Deutsche Forschungsgemeinschaft CRC 1076
758 “AquaDiva”. SZ acknowledges support from the European Research Council
759 (ERC) under the European Union’s Horizon 2020 research and innovation
760 programme (QUINCY; grant no. 647204).

761 **References**

- 762 Allard, V., Soussana, J.-F., Falcimagne, R., Berbigier, P., Bonnefond, J.,
763 Ceschia, E., D’hour, P., Hénault, C., Laville, P., Martin, C., Pinarès-
764 Patino, C., 2007. The role of grazing management for the net biome pro-
765 ductivity and greenhouse gas budget (co₂, {N₂O} and ch₄) of semi-natural
766 grassland. *Agriculture, Ecosystems & Environment* 121, 47 – 58.
- 767 Allison, S. D., Oct 2014. Modeling adaptation of carbon use efficiency in
768 microbial communities. *Frontiers in Microbiology* 5.
- 769 Allison, S. D., Vitousek, P. M., May 2005. Responses of extracellular enzymes
770 to simple and complex nutrient inputs. *Soil Biology & Biochemistry* 37 (5),
771 937–944.
- 772 Averill, C., Jul 2014. Divergence in plant and microbial allocation strategies
773 explains continental patterns in microbial allocation and biogeochemical
774 fluxes. *Ecology Letters* 17 (10), 1202–1210.
- 775 Averill, C., Rousk, J., Hawkes, C., Nov 2015. Microbial-mediated redistribu-
776 tion of ecosystem nitrogen cycling can delay progressive nitrogen limita-
777 tion. *Biogeochemistry* 126, 11–23.

- 778 Ballantyne, F., Billings, S., May 2014. Shifting resource availability, plastic
779 allocation to exoenzymes and the consequences for heterotrophic soil respi-
780 ration. In: EGU General Assembly Conference Abstracts. Vol. 16 of EGU
781 General Assembly Conference Abstracts. p. 16780.
782 URL <http://adsabs.harvard.edu/abs/2014EGUGA...1616780B>
- 783 Blagodatskaya, E., Khomyakov, N., Myachina, O., Bogomolova, I., Blago-
784 datsky, S., Kuzyakov, Y., Jul 2014. Microbial interactions affect sources of
785 priming induced by cellulose. *Soil Biology and Biochemistry* 74, 39–49.
- 786 Burns, R. G., DeForest, J. L., Marxsen, J., Sinsabaugh, R. L., Stromberger,
787 M. E., Wallenstein, M. D., Weintraub, M. N., Zoppini, A., 2013. Soil
788 enzymes in a changing environment: Current knowledge and future direc-
789 tions. *Soil Biology and Biochemistry* 58, 216 – 234.
- 790 Clarholm, M., Dec 1981. Protozoan grazing of bacteria in soil - impact and
791 importance. *Microbial Ecology* 7, 343–350.
- 792 Clarholm, M., 1985. Interactions of bacteria, protozoa and plants leading
793 to mineralization of soil nitrogen. *Soil Biology and Biochemistry* 17 (2),
794 181–187.
- 795 Cleveland, C. C., Liptzin, D., Aug 2007. C:n:p stoichiometry in soil: is there a
796 redfield ratio for the microbial biomass? *Biogeochemistry* 85 (3), 235–252.
- 797 Davidson, E. A., Samanta, S., Caramori, S. S., Savage, K., 2012. The dual
798 arrhenius and michaelis-menten kinetics model for decomposition of soil
799 organic matter at hourly to seasonal time scales. *Global Change Biology*
800 18 (1), 371–384.

- 801 Drake, J. E., Darby, B. A., Giasson, M.-A., Kramer, M. A., Phillips, R. P.,
802 Finzi, A. C., 2013. Stoichiometry constrains microbial response to root
803 exudation- insights from a model and a field experiment in a temperate
804 forest. *Biogeosciences* 10 (2), 821–838.
- 805 Drake, J. E., Gallet-Budynek, A., Hofmockel, K. S., Bernhardt, E. S.,
806 Billings, S. A., Jackson, R. B., Johnsen, K. S., Lichter, J., McCarthy, H. R.,
807 McCormack, M. L., Moore, D. J. P., Oren, R., Palmroth, S., Phillips, R. P.,
808 Pippen, J. S., Pritchard, S. G., Treseder, K. K., Schlesinger, W. H., DeLu-
809 cia, E. H., Finzi, A. C., 2011. Increases in the flux of carbon belowground
810 stimulate nitrogen uptake and sustain the long-term enhancement of forest
811 productivity under elevated CO₂. *Ecology Letters* 14 (4), 349357.
- 812 Fontaine, S., Henault, C., Aamor, A., Bdioui, N., Bloor, J., Maire, V., Mary,
813 B., Revailiot, S., Maron, P., Jan 2011. Fungi mediate long term seques-
814 tration of carbon and nitrogen in soil through their priming effect. *Soil*
815 *Biology and Biochemistry* 43 (1), 86–96.
- 816 Fontaine, S., Mariotti, A., Abbadie, L., Jun 2003. The priming effect of
817 organic matter: a question of microbial competition? *Soil Biology & Bio-*
818 *chemistry* 35 (6), 837–843.
- 819 Franklin, O., Näsholm, T., Högberg, P., Högberg, M. N., May 2014. Forests
820 trapped in nitrogen limitation - an ecological market perspective on ecto-
821 mycorrhizal symbiosis. *New Phytol* 203 (2), 657–666.
- 822 Friedlingstein, P., Meinshausen, M., Arora, V. K., Jones, C. D., Anav, A.,

823 Liddicoat, S. K., Knutti, R., 2014. Uncertainties in cmip5 climate projec-
824 tions due to carbon cycle feedbacks. *Journal of Climate* 27 (2), 511–526.

825 Janssens, I. A., Dieleman, W., Luyssaert, S., Subke, J.-A., Reichstein, M.,
826 Ceulemans, R., Ciais, P., Dolman, A. J., Grace, J., Matteucci, G., et al.,
827 Apr 2010. Reduction of forest soil respiration in response to nitrogen de-
828 position. *Nature Geosci* 3 (5), 315–322.

829 Kaiser, C., Franklin, O., Dieckmann, U., Richter, A., Mar 2014. Microbial
830 community dynamics alleviate stoichiometric constraints during litter de-
831 cay. *Ecol Lett* 17 (6), 680–690.

832 Kumar, A., Kuzyakov, Y., Pausch, J., Jun 2016. Maize rhizosphere priming:
833 field estimates using ^{13}C natural abundance. *Plant and Soil*.

834 Kuzyakov, Y., Friedel, J. K., Stahr, K., Oct 2000. Review of mechanisms and
835 quantification of priming effects. *Soil Biology & Biochemistry* 32 (11-12),
836 1485–1498.

837 Manzoni, S., Porporato, A., 2009. Soil carbon and nitrogen mineraliza-
838 tion: Theory and models across scales. *Soil Biology and Biochemistry* 41,
839 1355–1379.

840 Manzoni, S., Porporato, A., Schimel, J. P., May 2008. Soil heterogeneity in
841 lumped mineralization-immobilization models. *Soil Biology & Biochem-*
842 *istry* 40 (5), 1137–1148.

843 Moorhead, D. L., Lashermes, G., Sinsabaugh, R. L., 2012. A theoretical
844 model of c-and n-acquiring exoenzyme activities, which balances microbial

845 demands during decomposition. *Soil Biology and Biochemistry* 53, 133–
846 141.

847 Mooshammer, M., Wanek, W., Hämmerle, I., Fuchslueger, L., Hofhansl, F.,
848 Knoltsch, A., Schnecker, J., Takriti, M., Watzka, M., Wild, B., et al., Apr
849 2014a. Adjustment of microbial nitrogen use efficiency to carbon:nitrogen
850 imbalances regulates soil nitrogen cycling. *Nat Comms* 5.

851 Mooshammer, M., Wanek, W., Zechmeister-Boltenstern, S., Richter, A.,
852 2014b. Stoichiometric imbalances between terrestrial decomposer commu-
853 nities and their resources: mechanisms and implications of microbial adap-
854 tations to their resources. *Frontiers in Microbiology* 5.

855 Norby, R. J., Warren, J. M., Iversen, C. M., Medlyn, B. E., McMurtrie,
856 R. E., Sep. 2010. CO₂ enhancement of forest productivity constrained
857 by limited nitrogen availability. *Proceedings of the National Academy of*
858 *Sciences* 107 (45), 19368–19373.

859 Panikov, N. S., 2010. Microbial ecology. *Environmental Biotechnology*, 121–
860 191.

861 Perveen, N., Barot, S., Alvarez, G., Klumpp, K., Martin, R., Rapaport,
862 A., Herfurth, D., Louault, F., Fontaine, S., Apr 2014. Priming effect and
863 microbial diversity in ecosystem functioning and response to global change:
864 a modeling approach using the symphony model. *Glob Change Biol* 20 (4),
865 1174 – 1190.

866 Phillips, R. P., Finzi, A. C., Bernhardt, E. S., 2011. Enhanced root exudation

867 induces microbial feedbacks to n cycling in a pine forest under long-term
868 CO₂ fumigation. *Ecology Letters* 14 (2), 187194.

869 R Core Team, 2016. R: A Language and Environment for Statistical Com-
870 puting. R Foundation for Statistical Computing, Vienna, Austria.
871 URL <https://www.R-project.org>

872 Rastetter, E. B., Feb 2011. Modeling coupled biogeochemical cycles. *Frontiers*
873 in *Ecology and the Environment* 9 (1), 68 – 73.

874 Rastetter, E. B., Ågren, G. I., Shaver, G. R., May 1997. RESPONSES
875 OF n-LIMITED ECOSYSTEMS TO INCREASED CO₂: a BALANCED-
876 NUTRITION, COUPLED-ELEMENT-CYCLES MODEL. *Ecological Ap-*
877 *plications* 7 (2), 444–460.

878 Raynaud, X., Lata, J. C., Leadley, P. W., Sep 2006. Soil microbial loop and
879 nutrient uptake by plants: a test using a coupled c : N model of plant-
880 microbial interactions. *Plant and Soil* 287 (1-2), 95–116.

881 Resat, H., Bailey, V., McCue, L. A., Konopka, A., Dec 2011. Modeling mi-
882 crobial dynamics in heterogeneous environments: Growth on soil carbon
883 sources. *Microbial Ecology* 63 (4), 883–897.

884 Rousk, J., Hill, P. W., Jones, D. L., Dec 2014. Priming of the decomposition
885 of ageing soil organic matter: concentration dependence and microbial
886 control. *Functional Ecology* 29 (2), 285–296.

887 Schimel, J. P., Weintraub, M. N., 2003. The implications of exoenzyme ac-
888 tivity on microbial carbon and nitrogen limitation in soil: a theoretical
889 model. *Soil Biology and Biochemistry* 35, 549–563.

890 Sinsabaugh, R. L., Hill, B. H., Follstad Shah, J. J., Dec 2009. Ecoenzymatic
891 stoichiometry of microbial organic nutrient acquisition in soil and sediment.
892 Nature 462 (7274), 795–798.

893 Sinsabaugh, R. L., Manzoni, S., Moorhead, D. L., Richter, A., Jul 2013. Car-
894 bon use efficiency of microbial communities: stoichiometry, methodology
895 and modelling. Ecology Letters 16 (7), 930–939.

896 Sterner, R. W., Elser, J. J., 2002. Ecological stoichiometry: the biology of
897 elements from molecules to the biosphere. Princeton University Press.

898 Thornton, P. E., Lamarque, J.-F., Rosenbloom, N. A., Mahowald, N. M., Dec
899 2007. Influence of carbon-nitrogen cycle coupling on land model response
900 to co₂ fertilization and climate variability. Global Biogeochemical Cycles
901 21 (4).

902 Todd-Brown, K. E. O., Hopkins, F. M., Kivlin, S. N., Talbot, J. M., Allison,
903 S. D., Jul. 2012. A framework for representing microbial decomposition in
904 coupled climate models. Biogeochemistry 109 (1-3), 19–33.

905 van Bodegom, P., May 2007. Microbial maintenance: A critical review on its
906 quantification. Microbial Ecology 53 (4), 513–523.

907 Wang, G., Post, W. M., Mayes, M. A., Jan 2013. Development of microbial-
908 enzyme-mediated decomposition model parameters through steady-state
909 and dynamic analyses. Ecological Applications 23 (1), 255–272.

910 Wieder, W. R., Bonan, G. B., Allison, S. D., Jul 2013. Global soil carbon
911 projections are improved by modelling microbial processes. Nature Climate
912 Change.

- 913 Wutzler, T., Reichstein, M., 2008. Colimitation of decomposition by sub-
914 strate and decomposers - a comparison of model formulations. *Biogeo-*
915 *sciences* 5 (3), 749–759.
- 916 Wutzler, T., Reichstein, M., Mar. 2013. Priming and substrate quality inter-
917 actions in soil organic matter models. *Biogeosciences* 10 (3), 2089–2103.
- 918 Xu, X., Schimel, J. P., Thornton, P. E., Song, X., Yuan, F., Goswami, S.,
919 2014. Substrate and environmental controls on microbial assimilation of
920 soil organic carbon: a framework for earth system models. *Ecology letters*
921 17 (5), 547–555.
- 922 Xu, X., Thornton, P. E., Post, W. M., Jun 2013. A global analysis of soil mi-
923 crobial biomass carbon, nitrogen and phosphorus in terrestrial ecosystems.
924 *Global Ecology and Biogeography* 22 (6), 737–749.
- 925 Zaehle, S., Dalmonech, D., Oct. 2011. Carbon-nitrogen interactions on land
926 at global scales: current understanding in modelling climate biosphere
927 feedbacks. *Current Opinion in Environmental Sustainability* 3 (5), 311–
928 320.
- 929 Zechmeister-Boltenstern, S., Keiblinger, K. M., Mooshammer, M., Penuelas,
930 J., Richter, A., Sardans, J., Wanek, W., May 2015. The application of
931 ecological stoichiometry to plant - microbial - soil organic matter transfor-
932 mations. *Ecological Monographs* 85 (2), 133–155.